Supporting Information

Natural Polyphenol Fluorescent Polymer Dots

Peng Yang,[1, †] Xin Zhou,[1, †] Jianhua Zhang,[2] Jian Zhong,[3] Fang Zhu,[1] Xianhu Liu,[4] Zhipeng Gu,[1,*] and Yiwen Li[1,*]

[1] College of Polymer Science and Engineering, State Key Laboratory of Polymer Materials Engineering, Sichuan University, Chengdu 610065, China

[2] School of Materials Science and Engineering, Xihua University, Chengdu 610039, China

[3] State Key Laboratory of Biotherapy, West China Hospital, West China Medical School, Sichuan University, Chengdu 610041, China

[4] National Engineering Research Center for Advanced Polymer Processing Technology, Zhengzhou University, Zhengzhou 450002, China.

E-mail: ywli@scu.edu.cn (Y. L.), Tel: +86 028-85401066;
guzhipeng2019@scu.edu.cn (Z. G.), Tel: +86 028-85401066.

[†] These authors contributed equally to this work.

Materials

Tannic acid (TA), polyethyleneimine (PEI, 98%, Mw = 1800), ethylenediaminetetraacetic acid (EDTA, 98%), quinine sulfate (98%, suitable for fluorescence), and poly-L-lysine (Mw = 2000~5000) were purchased from Shanghai Aladdin Biochemical Technology Co., Ltd. (Shanghai, China). $CuCl_2 \cdot 2H_2O$ (99%), $MnCl_2 \cdot 4H_2O$ (99%), $MgCl_2 \cdot 6H_2O$ (98%), $CdCl_2 \cdot 2.5H_2O$ (98%), $FeCl_3$ (98%), $CoCl_2$ (98%), $AlCl_3$ (98%), KCl (99.5%), $CaCl_2$ (96%), NaCl (99.5%), Na_2S (98%), NaI (98%), Na_2SO_3 (97%), Na_2SO_4 (99%), Na_2CO_3 (99.8%), $NaH_2PO_4 \cdot 2H_2O$ (99%), $NaNO_3$ (98%), $NaHCO_3$ (99.5%), $NaHSO_3$ (98%), Na_2HPO_4 (99%), $CH_3COONa \cdot 3H_2O$ (99%) and Trihydroxyaminomethane (Tris, 99.5%) were acquired from Kelong Chemical Reagent Co., Ltd. (Chengdu, China). Histidine (99%), aspartic acid (99%), cysteine (98%), isoleucine (99%), serine (99%), alanine (99%), proline (99%), lysine (98%), threonine (99%), leucine (99%), methionine (99%), glycine (99%), tryptophan (99%), arginine (99%), glutamine (99%), valine (99%), tyrosine (99%), vitamin C (99%), glutamic acid (99%), glutathione (98%), albumin bovine V (98%), glucose (ACS reagent) and lecithin (98%) were purchased from J&K Chemical Ltd (Beijing, China). Epicatechin (EC, 98%), epigallocatechin gallate (EGCG, 98%), chlorogenic acid (98%), polyphenol extracts from red wine, apple, and pomegranate peel were obtained from Dasf biotechnology Co., Ltd. (Nanjing, China). Sodium borohydride ($NaBH_4$, 97%) was acquired from Kermel Chemical Reagent Co., Ltd. (Tianjin, China).

All reagents are freshly used as received in the studies.

Synthesis of natural polyphenol-based PDs

Four natural water-soluble polyphenols (tannic acid, epicatechin, epigallocatechin gallate, and chlorogenic acid) were selected. 200 mg natural polyphenols (e.g., tannic acid, TA) and 200 mg polyethyleneimine (PEI) (Mw=1800) were added into 50 mL Tris-HCl buffer (10 mM, pH 8.5). Subsequently, the mixture was stirred for 12 hours at room temperature. Afterward, the solution was filtered through a 0.22 μm membrane filters (polyether sulfone, Beijing Balb Technology Co. Ltd.), then dialyzed against 2L pure water through a dialysis bag (molecular weight cut-off 3500 Da) for 48 h. The synthesis and purification process of the products were both protected from light by a black cover. Finally, the obtained purified PDs were freeze-drying and stored away from light for further use.

Characterization

Transmission electron microscopy (TEM) images were performed on the FEI transmission electron microscope (F20). A Zetasizer Nano ZS (Nano ZS ZEN 3690) was applied to measure zeta potentials and size distribution. The UV-Vis absorption spectra were detected on a micro-spectrophotometer with a 1 cm quartz cell (PerkinElmer, Lambda 650). The organic element analyses were carried out on the Flash EA 1112. Fourier transform infrared spectroscopy (FTIR) was conducted on a Fourier Transform Infrared spectrometer (Perkin-Elmer spectrum one B system) using KBr pellets. Fluorescence spectra were recorded on the F98 fluorescence

spectrophotometer (Shanghai Lengguang Technology Co., Ltd.) with the excitation and emission slit width at 10 nm. The elemental composition of the sample surfaces was examined by X-ray photoelectron spectroscopy (PHI Quantera SXM spectrometer) using Al Kα X-ray radiation. Fluorescence lifetime was measured on a Fluorolog-3 spectrofluorometer (Horiba JobinYvon) with a DeltaDiode (406 nm, DD-405L) as the excitation source and a picosecond photon detection module (PPD-850) as the detector. ICP-OES results were determined by Agilent, ICP-OES 5100 SVDV. The samples need to be dissolved in ~ 1% nitric acid solution overnight before testing. The relative standard deviation (RSD) was obtained by repeating the experiments 3 times under the exact same experimental conditions.

Cyclic voltammogram (CV) measurements

CHI760E electrochemical workstation was employed to determine the E_g of PNs using indium tin oxide (ITO) coated with sample as the working electrode. Pt wire was as the counter electrode, and Ag/AgCl was as the reference electrode in a 0.1 M tetrabutylammonium hexafluorophosphate (Bu_4NPF_6) acetonitrile solution.

DFT calculation

Geometry optimizations in ground state and energy levels of the molecular orbits were determined by the Gaussian 09 package. The molecular orbits of possible moieties were imported at the B3LYP/6-31 G (d, p) level.

QY measurement of the PD-1

The QY of PD-1 is calculated via the following equation:

$$\varphi_x = \varphi_s \frac{k_x n_x^2}{k_s n_s^2}$$

where φ is the QY, k represents the slope of calibration plot obtained from the linear fitting curve of integrated fluorescence intensity against absorbance of different sample concentrations (A＜0.1), n represents the refractive index of the solvent. The subscripts x and s refer to the PD-1 and quinine sulfate, respectively. Quinine sulfate (literature φ=55% at 400 nm) was dissolved in 0.1M H_2SO_4 (n=1.33) while PD-1 were dispersed in distilled water (n=1.33).

Fluorescence determination of Cu^{2+}

The fluorescence determination of Cu^{2+} was carried out as the following procedure. The PD-1 (100 μL, 1.5 mg/mL) were added to the Cu^{2+} solutions (200 μL) with different concentrations (0-200 μM). Then, the emission spectra (440–650 nm) were measured (E_x=400nm) with the excitation and emission slit width at 10 nm. The fluorescence intensities of the PD-1 with and without the addition of Cu^{2+} were represented as F and F_0, respectively.

Cell culture, cytocompatibility test and cell imaging

NIH 3T3 cells and A549 cells were cultured in Dulbecco's modified Eagle's medium (DMEM) supplemented with 10% fetal bovine serum (FBS) and 100 units/mL penicillin and 100 mg/mL streptomycin in a humidified incubator with 5% CO_2 at 37

°C. For the cytotoxicity test, the cell viability was evaluated by the Alamar blue assay. Taking NIH 3T3 cells as the example, the cells were seeded in 96-well plate and incubated for 12 h (5000 cells/well). Then, the cells were treated with the PD-1 at different concentrations. After another 24 h, the cell viability was measured using standard Alamar blue assay. For the imaging, NIH 3T3 cells were seeded in petri dishes with a glass bottom and incubated for 24 h (3.0×10^5 cells per dish). Then the medium was removed and replaced with a new medium with the PD-1 at different concentrations. After another 8 h, the medium was removed and washed with PBS buffer for three times. For the sensing Cu^{2+}, the cells were treated with saline containing 20 μM of Cu^{2+} for 1 h subsequently, and then washed with PBS buffer for three times. The fluorescence images were recorded by a confocal laser with excitation at 405 nm (ZEISS LSM880). The mean fluorescence intensity was determined by the software (ZEN blue).

Detection of Cu^{2+} in real water samples.

The real water samples were collected from Jin River and Dong Lake (Chengdu, Sichuan Province, China). Taking the sample from Jin River as the example, the sample was first centrifuged and filtered twice to remove suspended solids before use. Then, the sample was added $CuCl_2$ and the final concentration was determined by ICP-OES. Cu^{2+} concentration of the sample was also measured by the PDs sensing technique and compared with the result obtained from ICP-OES. The relative standard deviation (RSD) was obtained by repeating the experiments 3 times under the same experimental

conditions.

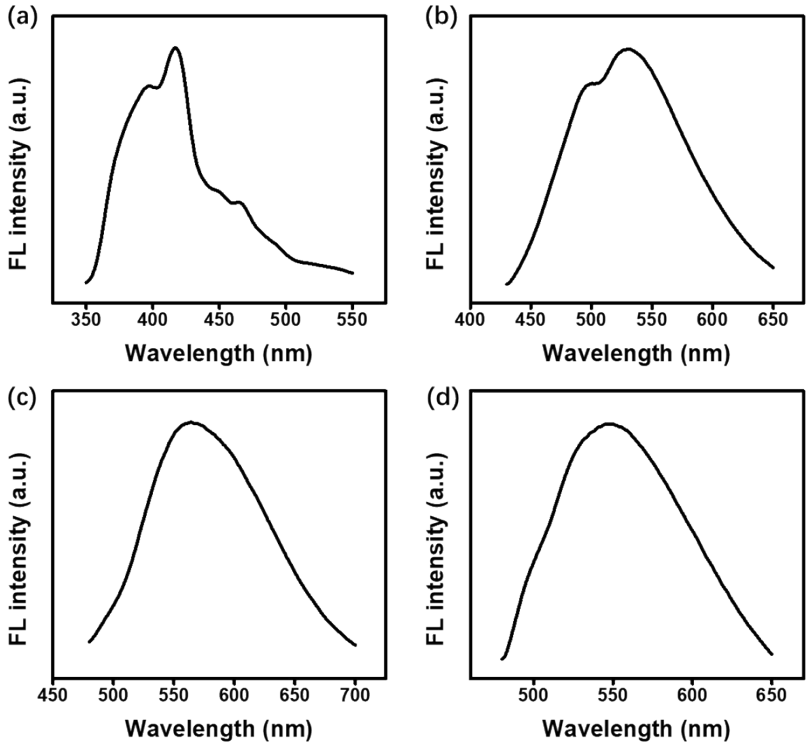

Fig. S1. The fluorescence spectra of the products from (a) TA with poly-L-lysine, natural polyphenol extract from (b) red wine, (c) apple, and (d) pomegranate peel with PEI, respectively.

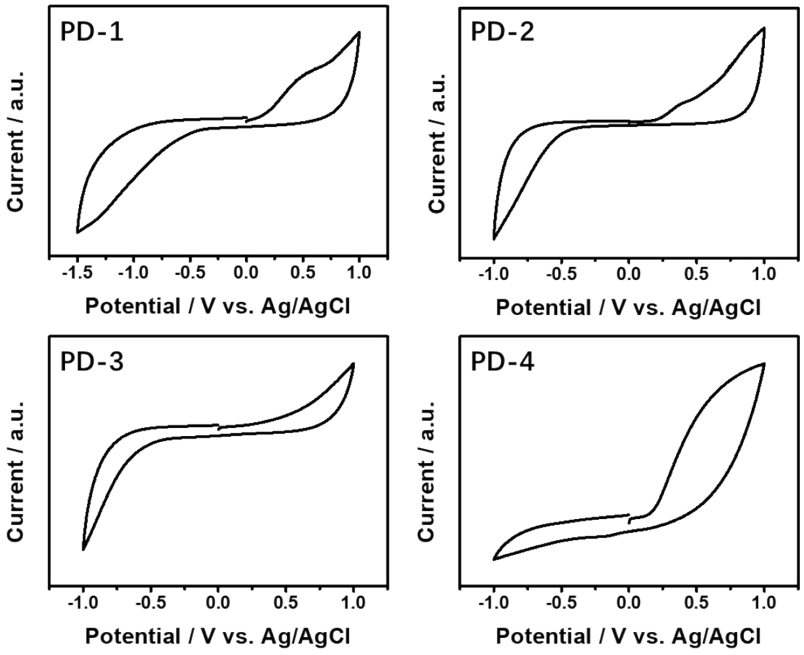

Fig. S2. Cyclic voltammograms of PDs.

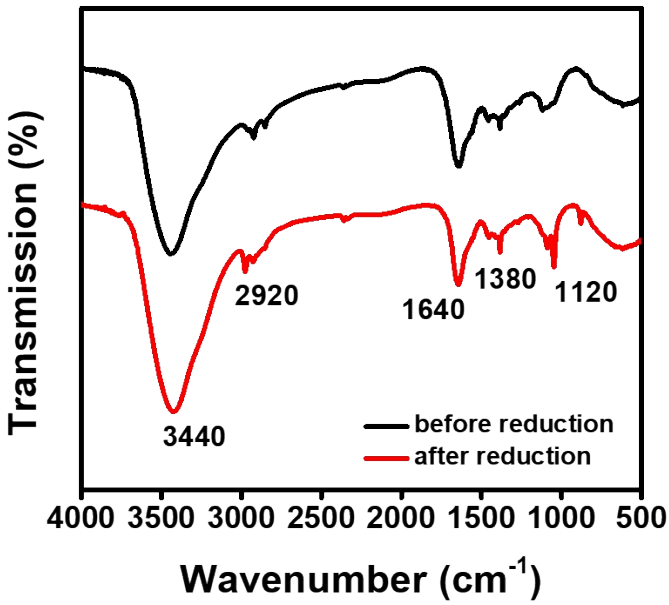

Fig. S3. FT-IR spectra of the PD-1 before and after reduction.

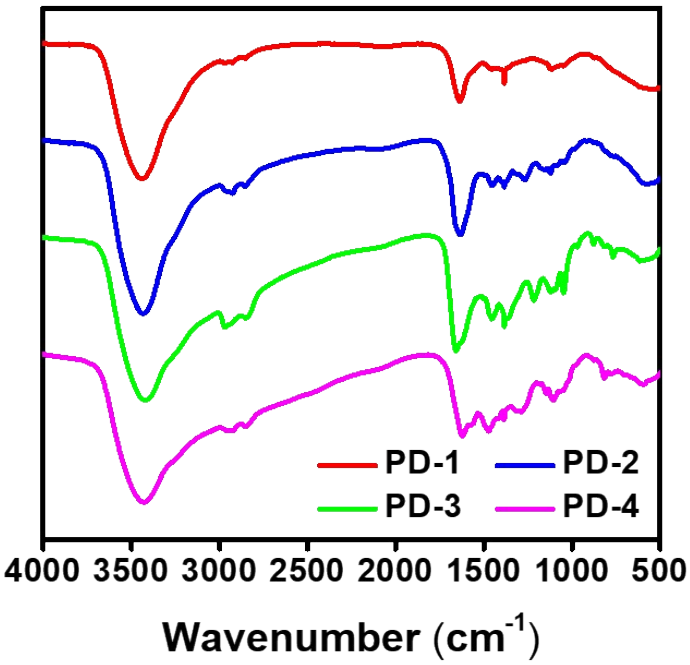

Fig. S4. FT-IR spectra of PD-i (i=1-4).

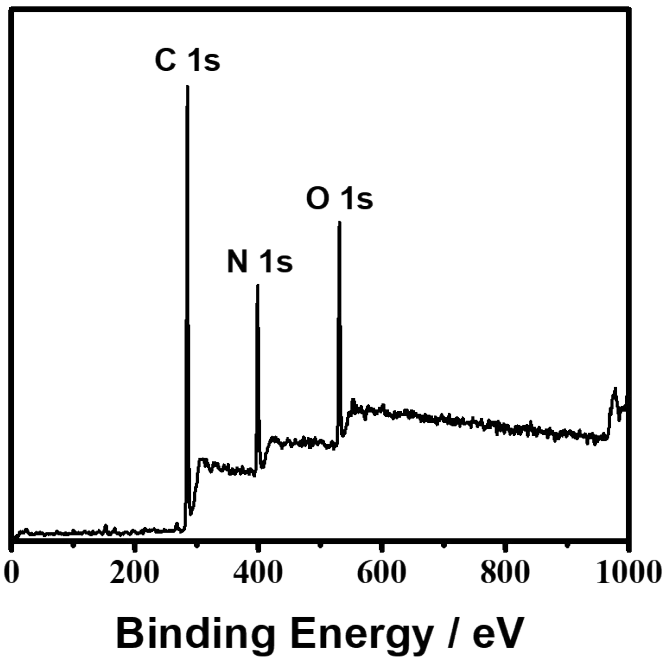

Fig. S5. X-ray photoelectron spectrum of the PD-1.

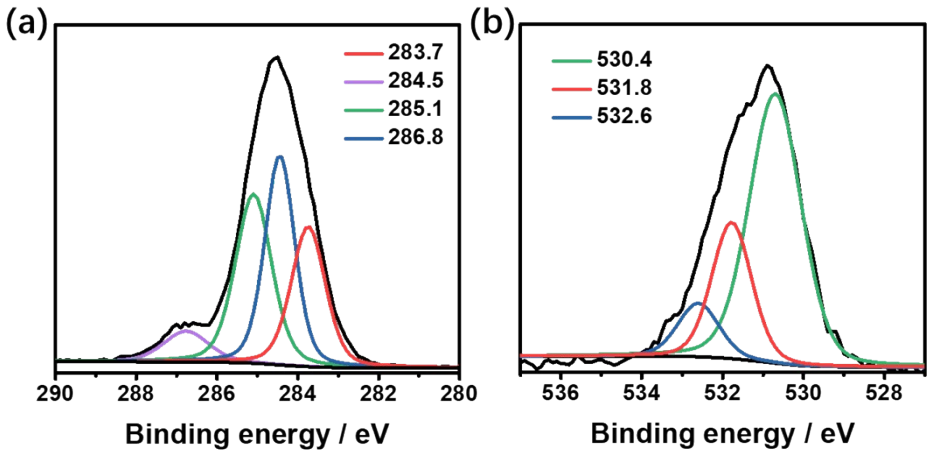

Fig. S6. XPS spectra of C 1s (a) and O 1s (b) regions of the PD-1.

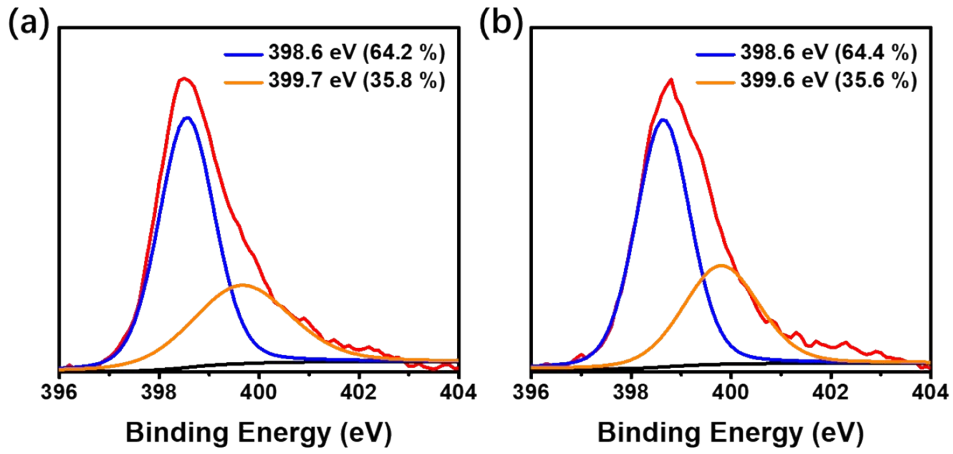

Fig. S7. XPS spectra of N 1s regions of the PD-1 before (a) and after (b) reduction.

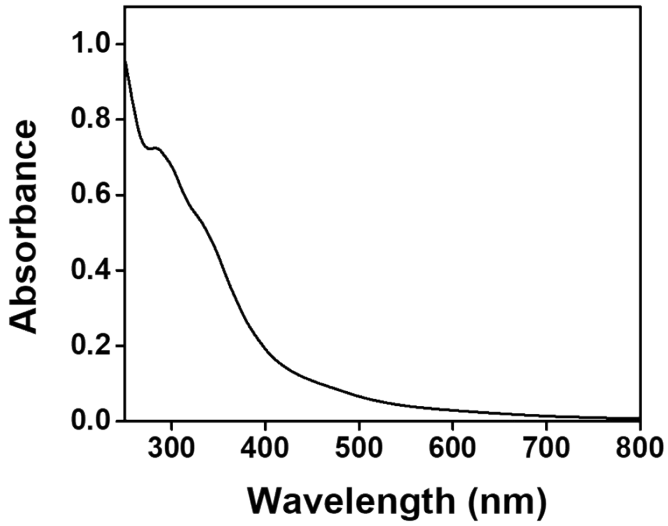

Fig. S8. The UV-Vis spectrum of PD-1.

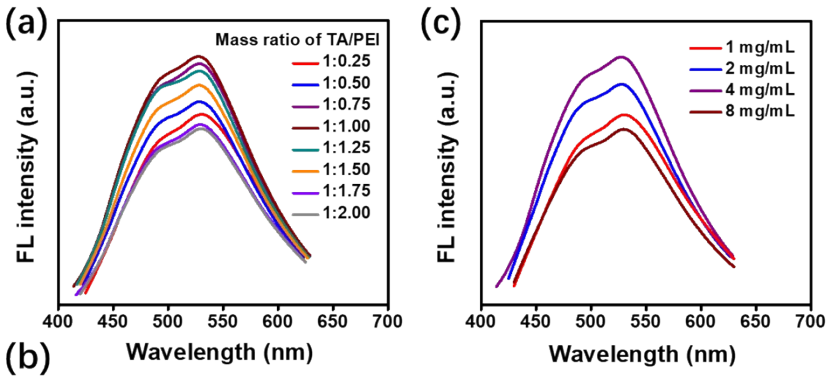

(b)

m_{TA} (mg)	m_{PEI} (mg)	Mass ratio of TA/PEI	Tris-HCl (mL)
200	50	1:0.25	50
	100	1:0.50	
	150	1:0.75	
	200	1:1.00	
	250	1:1.25	
	300	1:1.50	
	350	1:1.75	
	400	1:2.00	

Fig. S9. (a) The effect of the TA/PEI ratio on the fluorescence properties of the PD-1 keeping the TA concentration at 4 mg/mL. (b) The reaction conditions of TA/PEI system with different PEI mass in (a). (c) The effect of the TA/PEI concentration on the fluorescence intensity with the mass ratio of 1:1.

(a)

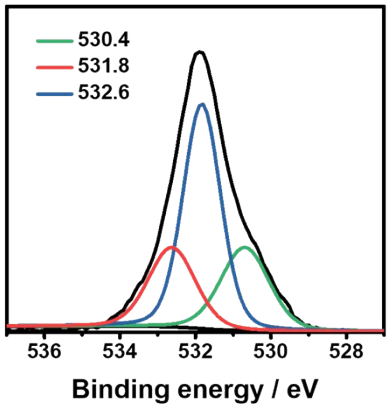

(b)

Binding energy	Content (before reduction)	Content (after reduction)
530.4 eV	63.79 %	25.15 %
531.8 eV	23.82 %	45.63 %
532.6 eV	12.39 %	29.22 %

Fig. S10. (a) XPS spectra of O 1s regions of the PD-1 after reduction. (b) The proportion of different bonds in the O 1s regions.

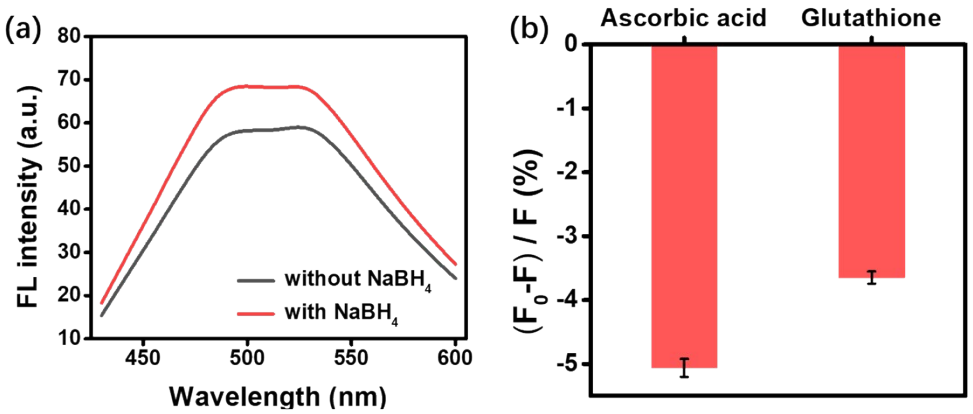

Fig. S11. (a) The fluorescence spectra of the PD-1 before and after $NaBH_4$ treatment.

(b) The fluorescence change of the PD-1 after ascorbic acid and glutathione treatment.

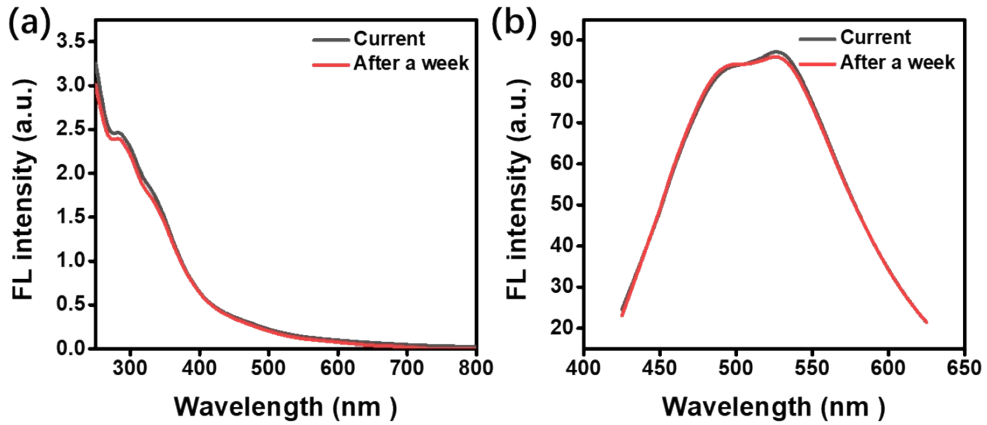

Fig. S12. The changes of UV-Vis spectra (a) and fluorescence spectra (b) of the PD-1 after a week.

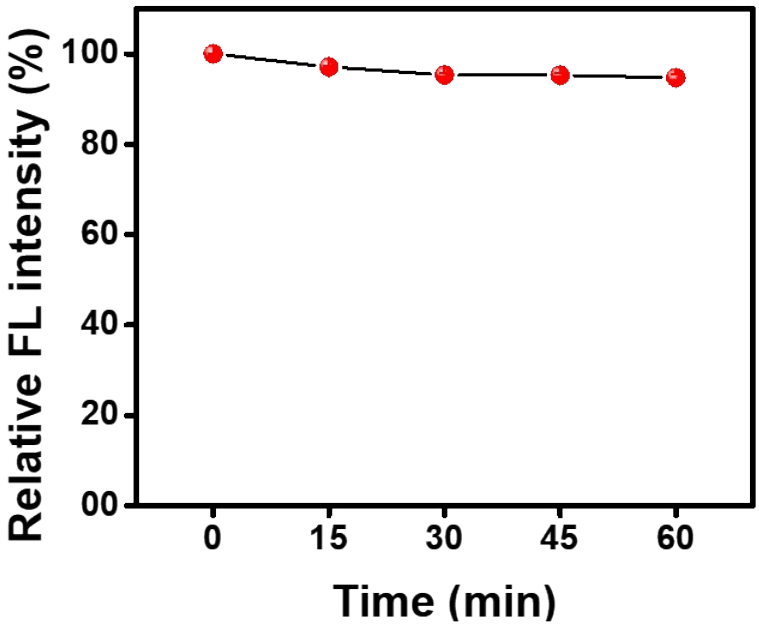

Fig. S13. The relative fluorescence intensity of the PD-1 under continuous excitation (365 nm, 12W).

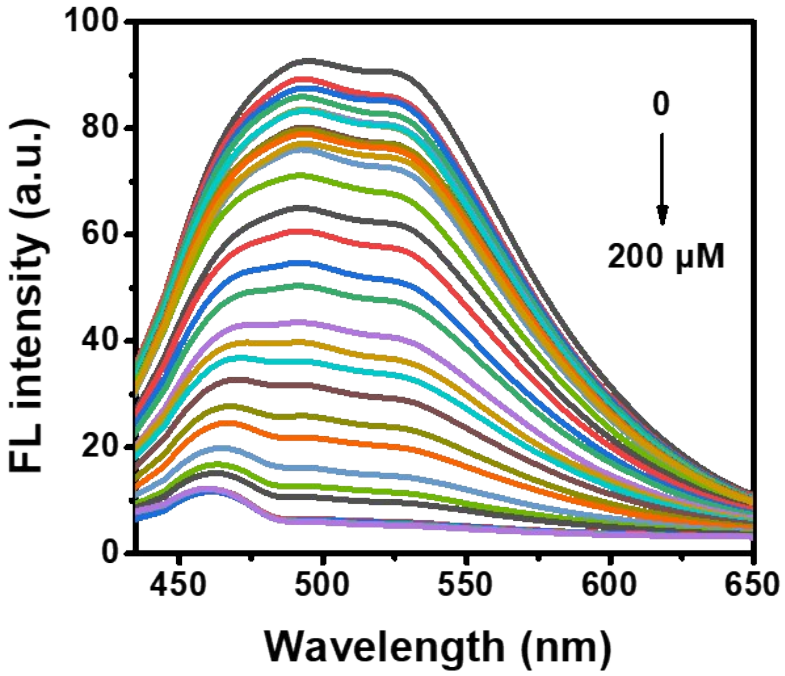

Fig. S14. Fluorescence intensity change of the PD-1 with the increasing of Cu^{2+} concentration.

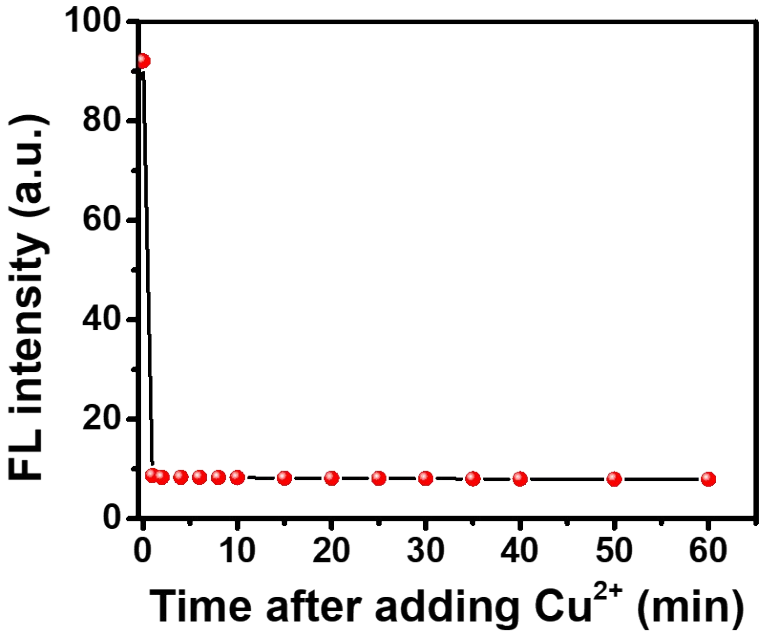

Fig. S15. Fluorescence intensity of PD-1 after addition Cu^{2+} as a function of time.

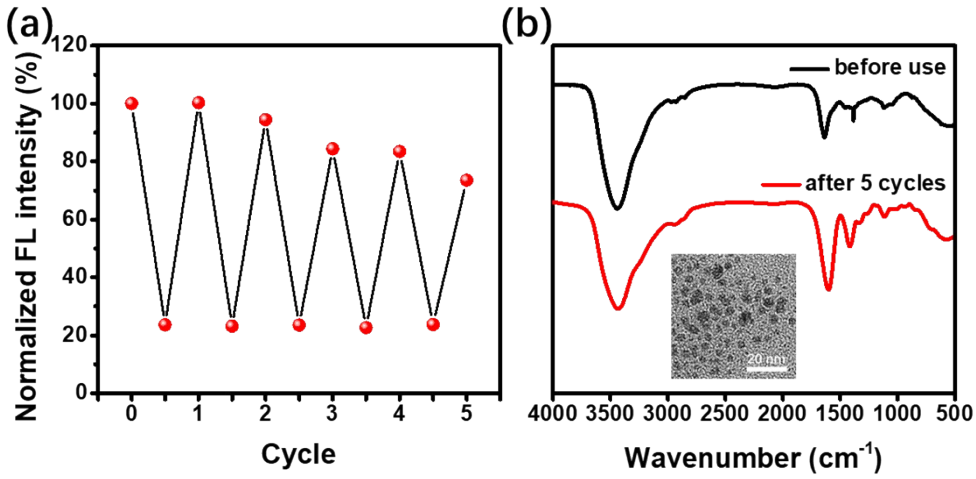

Fig. S16. (a) Reversible switching of PD-1 fluorescence by alternately adding Cu^{2+} and EDTA. (b) FT-IR spectra of the PD-1 before use and after 5 cycles. Inset is the TEM image of PD-1 after 5 cycles.

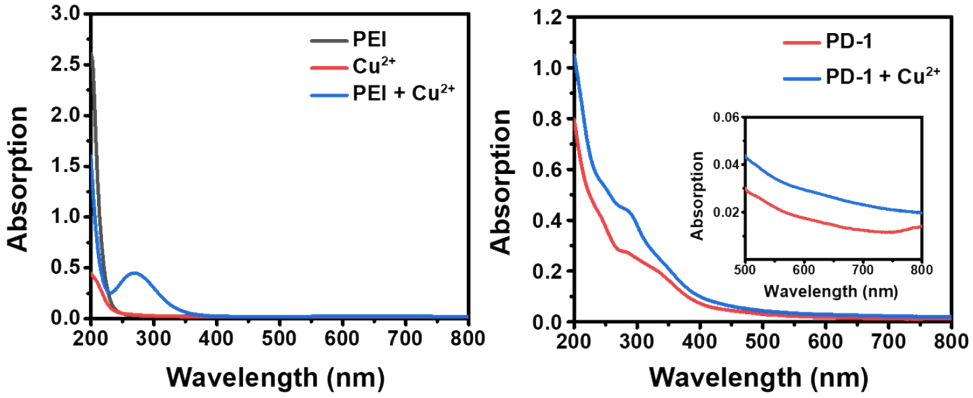

Fig. S17. (a) The UV-Vis spectra of PEI, Cu^{2+}, and PEI+Cu^{2+}. (b) UV-Vis spectra change of the PD-1 in the absence and the presence of Cu^{2+}.

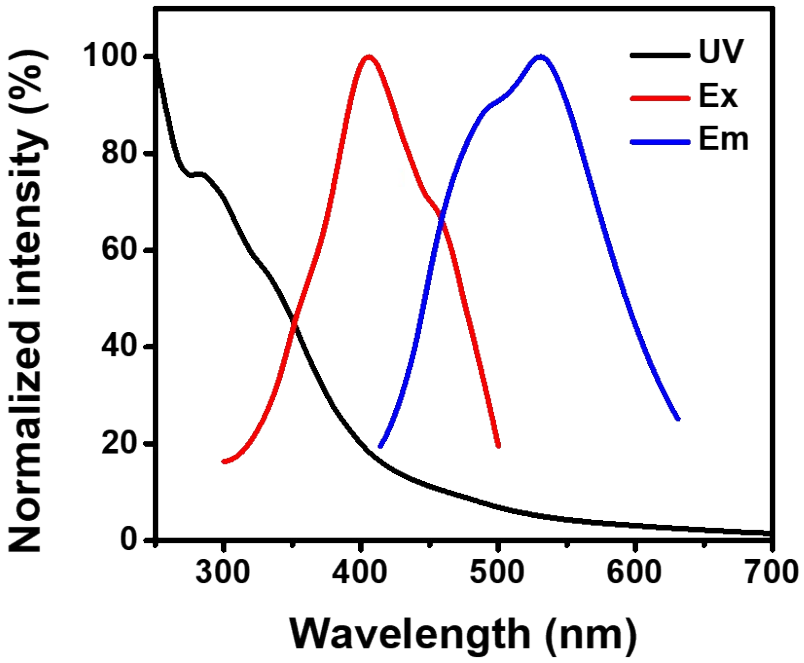

Fig. S18. The normalized UV spectrum and FL spectra (excitation spectrum and emission spectrum) of PD-1.

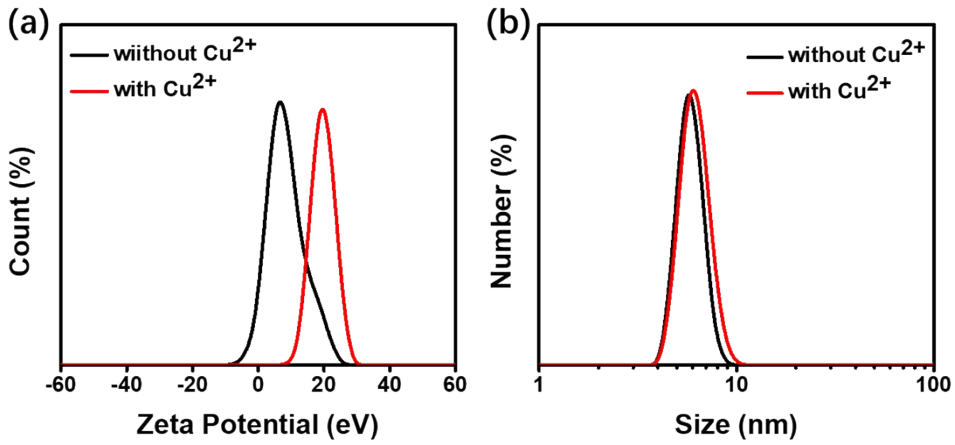

Fig. S19. (a) The zeta potential change of the PD-1 after adding Cu^{2+}. (b) The size distribution change of the PD-1 after adding Cu^{2+}.

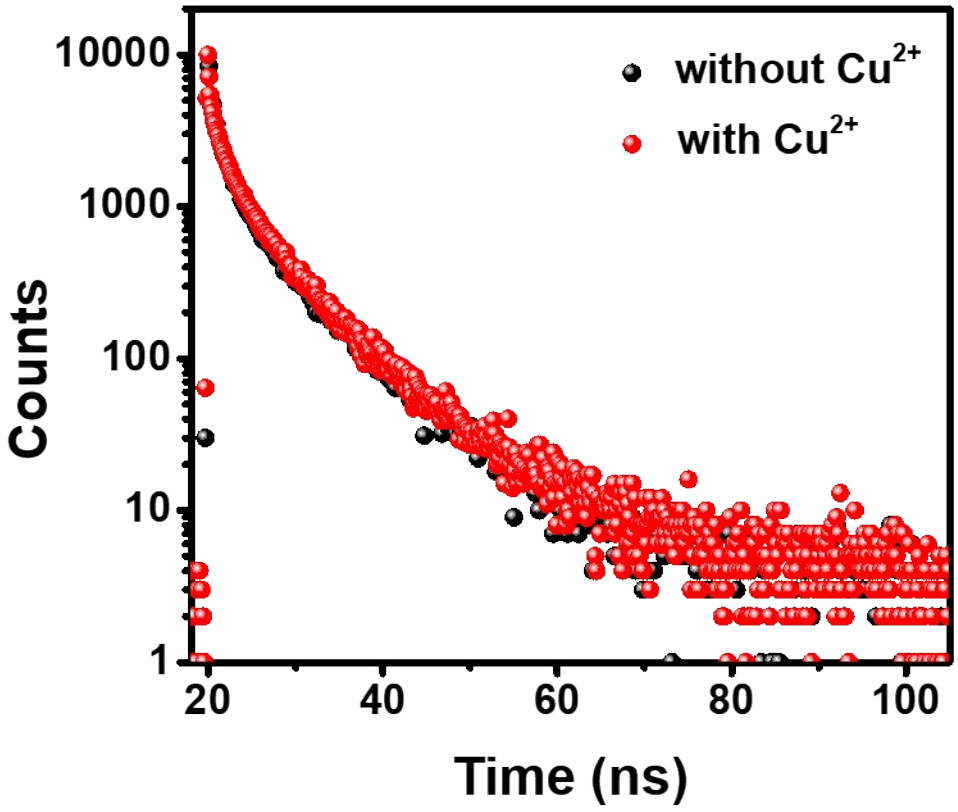

Fig. S20. Fluorescence lifetime change of the PD-1 in the absence and presence of Cu^{2+}.

Table S1. The yield, polyphenol content, and PEI content of each sample.

Sample	Yield (%)	N content (%)	Polyphenol content (%)	PEI content (%)
PD-1	7.5	17.1	47.4	52.6
PD-2	15.0	16.1	50.5	49.5
PD-3	5.1	14.9	54.2	45.8
PD-4	32.7	14.6	61.8	38.2

The polyphenols content and PEI content in the final products were calculated by the following equation, where the N contents were determined by the organic analysis.

$$(1 - x) \times N_{PEI} = N_{PD-i}$$

where x is the polyphenol content, N_{PEI} is calculated to be 32.5% by the chemical formula, and N_{PD-i} is the N content of PD-i (i=1-4).

Table S2. QY of various PDs.

Ref.	Precursors	Methods	QY / %	Years
[1]	PEI	Microwave	7.1	2017
[2]	PEI and salicylaldehyde	Self-assembly	4.6	2017
[3]	PEI and chitosan	Microwave	3.68	2018
[4]	PEI and $HAuCl_4$	Refluxed	1.5	2018
[5]	PEI and glutathione	Hydrothermal	2.7	2018
[6]	PEI and L-ascorbic acid	Self-assembly	3.1	2019
[7]	Tannic acid	Hydrothermal	6.9	2015
[8]	Tannic acid	Hydrothermal	7.16	2016
[9]	Tannic acid	Microwave	7.6	2016
[10]	Tannic acid and PEI	Microwave	0.1	2019

Reference

1. J. Wang, R. Sheng Li, H. Zhi Zhang, N. Wang, Z. Zhang and C. Z. Huang, *Biosens. Bioelectron.*, 2017, **97**, 157-163.
2. S. G. Liu, T. Liu, N. Li, S. Geng, J. L. Lei, N. B. Li and H. Q. Luo, *J. Phys. Chem. C*, 2017, **121**, 6874-6883.
3. S. Li, Z. Guo, G. Zeng, Y. Zhang, W. Xue and Z. Liu, *ACS Biomaterials Science & Engineering*, 2017, **4**, 142-150.
4. N. Wang, Y. Liu, Y. Li, Q. Liu and M. Xie, *Sens. Actuators, B*, 2018, **255**, 78-86.
5. D. Luo, S. G. Liu, N. B. Li and H. Q. Luo, *Mikrochim. Acta*, 2018, **185**, 284.

6. Y. Chen, Y. Zhang, T. Lyu, Y. Wang, X. Yang and X. Wu, *J. Mater. Chem. C*, 2019, **7**, 9241-9247.
7. X. An, S. Zhuo, P. Zhang and C. Zhu, *RSC Advances*, 2015, **5**, 19853-19858.
8. Z. X. Liu, Z. L. Wu, M. X. Gao, H. Liu and C. Z. Huang, *Chem. Commun. (Camb.)*, 2016, **52**, 2063-2066.
9. J. Joseph and A. A. Anappara, *New J. Chem.*, 2016, **40**, 8110-8117.
10. T. Nozaki, T. Kakuda, Y. B. Pottathara and H. Kawasaki, *Photochem. Photobiol. Sci.*, 2019, **18**, 1235-1241.